Dimension Increase via Hydrogen Bonding and Weak Coordination Interactions from Simple Complexes of 2-(Pyridyl)benzimidazole Ligands

ARTICLE *in* CRYSTAL GROWTH & DESIGN · NOVEMBER 2007

Impact Factor: 4.89 · DOI: 10.1021/cg070080j

7 AUTHORS, INCLUDING:

Sheng-Run Zheng
South China Normal University
91 PUBLICATIONS **989** CITATIONS
SEE PROFILE

Qi-Ting He
South University of Science and Technolog…
4 PUBLICATIONS **107** CITATIONS
SEE PROFILE

CRYSTAL GROWTH & DESIGN
2007
VOL. 7, NO. 12
2481–2490

Dimension Increase via Hydrogen Bonding and Weak Coordination Interactions from Simple Complexes of 2-(Pyridyl)benzimidazole Ligands

Xiang-Ping Li,[†] Mei Pan,[†] Sheng-Run Zheng,[†] Yong-Ru Liu,[†] Qi-Ting He,[†] Bei-Sheng Kang,[†] and Cheng-Yong Su*[,†,‡]

MOE Laboratory of Bioinorganic and Synthetic Chemistry, State Key Laboratory of Optoelectronic Materials and Technologies, School of Chemistry and Chemical Engineering, Sun Yat-Sen University, Guangzhou 510275, and State Key Laboratory of Organometallic Chemistry, Shanghai Institute of Organic Chemistry, Chinese Academy of Sciences, Shanghai 200032, China

Received January 24, 2007; Revised Manuscript Received September 2, 2007

ABSTRACT: Two asymmetric ligands, 2-(3-pyridyl)benzimidazole (3-PyBim) and 2-(4-pyridyl)benzimidazole (4-PyBim) which are positional isomers and versatile to provide both coordination donors (N_{Py} and N_{Bim}) and hydrogen bonding sites (N_{Bim} and HN_{Bim}), were utilized to synthesize a series of transition metal complexes, namely $[Ag_2(3\text{-PyBim})_2](X)_2$ (X = BF_4^- (**1**), NO_3^- (**2**), ClO_4^- (**3**), $CF_3SO_3^-$ (**4**)), $[Ag(4\text{-PyBim})](NO_3)\cdot(H_2O)$ (**5**), $[Cu(3\text{-PyBim})_2(H_2O)_2](ClO_4)_2$ (**6**), $[Co(3\text{-PyBim})_2(H_2O)_4](NO_3)_2\cdot(H_2O)_4$(**7**), $[Cu(4\text{-PyBim})_2(Cl)_2](H_2O)_2$ (**8**), $[Zn(4\text{-PyBim})_2(H_2O)_2(NO_3)_2]$ (**9**), and $[Cu_2(3\text{-PyBim})_2(OAc)_4]$ (**10**). These simple complexes show diversified intermolecular interaction modes and can behave as basic structural units to be assembled into higher dimensional structures via dimension increasing. In complexes **1**–**4**, every two Ag (I) atoms are connected by two 3-PyBim ligands to form a discrete $[Ag_2(PyBim)_2]^{2+}$ cyclic unit, while in complex **5**, Ag (I) atoms are bridged by 4-PyBim ligands into a one-dimensional "zigzag" chain. This is due to positional isomerization of the ligands 3-PyBim and 4-PyBim, but they both display the similar end-to-end coordination mode. In contrast, these two ligands show the end-on coordination mode in complexes **6**–**9** with the Cu (II), Co (II), or Zn (II) ions taking on square or octahedral coordination geometries to form monomeric structural units containing one metal and two ligands, as well as additional water molecules or counteranions wherever necessary. In complex **10**, the well-known dimetal paddle-wheel motif is formed with two Cu (II) ions adopting a square pyramidal geometry, but the two 3-PyBim ligands also take the same end-on coordination mode as that in complexes **6**–**9**. The different coordination modes of the ligands in together with the influences from the counteranions play essential roles to propagate these basic structural units into 1D (**1**, **10**), 2D (**2**–**6**, **8**), or 3D (**7**, **9**) frameworks via hydrogen bonding and other weak interactions. Thermogravimetric properties of some complexes were also measured.

Introduction

Crystal engineering of coordination polymers and organic–inorganic hybrid materials aims at predictable and controllable synthesis of infinite one-, two- and three-dimensional (1D, 2D, and 3D) metal−organic supramolecular architectures for solid materials with predefined structures and properties.[1] The past few decades have witnessed tremendous progress in the self-assembly of elaborately designed building units by the aid of various kinds of intermolecular weak interactions such as hydrogen bonding, $\pi-\pi$ stacking, metal−metal interactions, and metal−nonmetal interactions.[2–4] The delicate balance between the adaptability of the building blocks and the synergistic effects of all these weak interactions accounts for the fact that the structure and topology of final complexes can be astonishingly varied even with the similar ligands.

The ligands containing 2-substituted benzimidazoles (2-Bim) have attracted considerable interest for their wide-ranging antiviral activities,[5] photochemical and photophysical properties,[6] versatile coordination modes, and potential to form supramolecular aggregates through $\pi-\pi$ stacking and hydrogen bonding.[7] We have been working on the supramolecular synthesis of various coordination assemblies containing benzimidazole and its derivatives and have reported a series of symmetric ditopic or tripodal 2-benzimidazolyl containing ligands and their complexes.[8] By contrast, studies on complexes with asymmetric ligands consisting of 2-benzimidazole and pyridine are relatively insufficient.[9] Herein, we report ten complexes assembled from two simple asymmetric ligands: 2-(3-pyridyl)benzimidazole (3-PyBim) and 2-(4-pyridyl)benzimidazole (4-PyBim). These two ligands coordinate with different metal ions in different ways and provide primary low-dimensional building units which further propagate into 1D, 2D, or 3D structures via hydrogen bonds and other intermolecular weak interactions.

Experimental Section

Materials and Method. All chemicals were of reagent grade obtained from commercial sources and used without further purification. The ligand 3-PyBim was prepared by a procedure similar to that reported for 1,3-bis(1-ethylbenzimidazol-2-yl)benzene,[10] and the ligand 4-PyBim was prepared according to the literature method.[11] The C, H, N elemental analyses were performed on a Perkin-Elmer 240 elemental analyzer. IR spectra were recorded on a Bruker Tensor 27 FT-IR spectrophotometer using KBr discs in the 4000–400 cm^{-1} region. Thermogravimetric analysis was carried out on a NETZSCH TG 209 instrument under air by heating the sample from 20 to 700 °C with a heating rate of 10 °C/min.

Synthesis and Characterization. The complexes **1** and **2**, $[Ag_2(3\text{-PyBim})_2](X)_2$ (X = BF_4^- (**1**), NO_3^- (**2**)), were prepared by a similar procedure. A solution of AgX (0.1 mmol) in CH_3CN (2 mL) was carefully layered onto a solution of 3-PyBim (0.02 g, 0.1 mmol) in mixed $CHCl_3-CH_3COCH_3$(5 mL, v/v = 1:1) in a test tube. The solution was left to stand for 5 days at room temperature in the dark, and colorless block crystals suitable for X-ray diffraction (XRD) analyses were obtained. Anal. calcd for $C_{24}H_{18}Ag_2B_2F_8N_6$ (**1**): C, 36.97; H, 2.33;

* Corresponding author. Fax: (+86) 20-8411-5178. E-mail: cesscy@mail.sysu.edu.cn.
[†] Sun Yat-Sen University.
[‡] Shanghai Institute of Organic Chemistry.

10.1021/cg070080j CCC: $37.00
Published on Web 11/15/2007

Table 1. Crystallographic Data for Complexes 1–10

	1	2	3	4	5
formula	$C_{24}H_{18}Ag_2B_2F_8N_6$	$C_{12}H_9AgN_4O_3$	$C_{24}H_{18}Ag_2Cl_2N_6O_8$	$C_{13}H_9AgF_3N_3O_3S$	$C_{12}H_{11}AgN_4O_4$
M_w	779.80	365.10	805.08	452.16	383.12
crystal system	monoclinic	triclinic	triclinic	monoclinic	orthorhombic
space group	*P*2(1)/*c*	*P*-1̄	*P*-1̄	*P*2(1)/*c*	*Aba*2
a, Å	10.374	8.314	8.238(2)	10.774(2)	18.125(2)
b, Å	10.122	9.078	9.466(2)	16.613(2)	13.0397(15)
c, Å	12.521	9.898	9.944(2)	8.481(4)	11.0126(12)
α, deg	90.00	106.08	107.55(3)	90.00	90.00
β, deg	96.62	96.76	106.65(3)	98.97	90.00
γ, deg	90.00	116.83	105.25(3)	90.00	90.00
V, Å^3	1306.0	614.4	654.5(2)	1499.4(8)	2602.7(5)
Z	2	2	1	4	8
D_c, (g cm^{-3})	1.983	1.974	2.043	2.003	1.955
μ (mm^{-1})	1.585	1.654	1.763	1.536	1.572
T (K)	293	293	293	293	293
R_1	0.0241	0.0311	0.0613	0.0660	0.0208
wR_2	0.0623	0.0844	0.1759	0.1483	0.0517
S	1.088	1.049	1.046	1.028	1.002

	6	7	8	9	10
formula	$C_{24}H_{22}Cl_2CuN_6O_{10}$	$C_{12}H_{17}Co_{0.5}N_4O_7$	$C_{24}H_{22}Cl_2Cu\ N_6O_2$	$C_{24}H_{22}N_8O_8Zn$	$C_{16}H_{15}CuN_3O_4$
M_w	688.92	358.76	560.92	615.87	376.85
crystal system	monoclinc	triclinic	monoclinic	triclinic	triclinic
space group	*P*2(1)/*c*	*P*-1̄	*P*2(1)/*c*	*P*-1̄	*P*-1̄
a, Å	10.714(2)	7.6579(16)	7.0234	7.426	8.148
b, Å	16.729(2)	9.948(2)	11.5342	8.957	9.688
c, Å	7.669(3)	11.140(2)	14.1741	9.773	11.095
α, deg	90.00	86.299(4)	90.00	97.17	103.06
β, deg	96.50	71.545(4)	100.793	105.17	97.85
γ, deg	90.00	81.353(4)	90.00	90.86	104.11
V, Å^3	1365.7(6)	795.8(3)	1127.9(2)	621.7	810.2
Z	2	2	2	1	2
D_c, (g cm^{-3})	1.675	1.497	1.652	1.645	1.545
μ (mm^{-1})	1.064	0.618	1.243	1.056	1.373
T (K)	293	293	293	293	293
R_1	0.0494	0.0504	0.0347	0.0272	0.0322
wR_2	0.1227	0.1296	0.0832	0.0766	0.0914
S	0.999	1.068	1.036	1.049	1.036

N, 10.78. Found: C, 36.46; H, 2.23; N, 10.39%. Anal. calcd for $C_{24}H_{18}Ag_2N_8O_6$ (**2**): C, 39.48; H, 2.48; N, 15.34. Found: C, 39.44; H, 2.63; N, 15.37%. IR (KBr, cm^{-1}): 3437m, 1618w, 1389s, 1319m, 1204w, 1136w, 1037w, 982w, 818w, 751w, 699w, 636w.

The complexes $[Ag_2(3\text{-PyBim})_2](ClO_4^-)_2$ (**3**), $[Ag_2(3\text{-PyBim})_2](CF_3SO_3^-)_2$ (**4**), and $[Cu(3\text{-PyBim})_2(H_2O)_2](ClO_4)_2$ (**6**) were prepared in a similar procedure[9b] as that above by using a mixed MeCN−MeOH solution instead of a $CHCl_3-CH_3COCH_3$ solution (5 mL, v/v = 1:1).

[Ag(4-PyBim)](NO$_3$)(H$_2$O) (5). A solution of $AgNO_3$(0.017 g, 0.1 mmol) in CH_3CN (2 mL) was carefully layered onto a solution of 4-PyBim (0.02 g, 0.1 mmol) in mixed $CHCl_3-CH_3OH$ (5 mL, v/v = 1:1) in a test tube. The solution was left to stand for several weeks at room temperature, and colorless crystals were obtained. Anal. calcd for $C_{12}H_{11}AgN_4O_4$: C, 37.62; H, 2.38; N, 14.62. Found: C, 38.04; H, 3.06; N, 14.81%. IR (KBr, cm^{-1}): 3437m, 1615m, 1384s, 1330m, 1231w, 1135w, 1011w, 829w, 775w, 699w, 564w.

[Co(3-PyBim)$_2$(H$_2$O)$_4$](NO$_3$)$_2$·(H$_2$O)$_4$ (7). A solution of $Co(NO_3)_2\cdot 6H_2O$ (0.029 g, 0.1 mmol) and 3-PyBim (0.02 g, 0.1 mmol) in CH_3COCH_3 (10 mL) was stirred for 10 min and filtered out. The clear filtrate was left in a beaker flask, and slow evaporation of the solvents resulted in precipitation of red crystals. Anal. calcd for $C_{12}H_{17}Co_{0.50}N_4O_7$: C, 40.63; H, 4.78; N, 15.79. Found: C, 40.72; H, 4.62; N, 15.28%. IR (KBr, cm^{-1}): 3218b, 1632m, 1373s, 1119w, 1047w, 969w, 749s, 566w.

[Cu(4-PyBim)$_2$ (Cl)$_2$](H$_2$O)$_2$ (8). A solution of $CuCl_2\cdot 2H_2O$ (0.017 g, 0.1 mmol) in CH_3CN (2 mL) was carefully layered onto a solution of 3-PyBim (0.02 g, 0.1 mmol) in mixed $CHCl_3-CH_3OH$ (5 mL, v/v = 1:1) in a test tube. The solution was left to stand for several weeks at room temperature, and green crystals were obtained. Anal. calcd for $C_{24}H_{22}Cl_2CuN_6O_2$: C, 51.39; H, 3.95; N, 14.98. Found: C, 51.50; H, 3.86; N, 15.06%. IR (KBr, cm^{-1}): 3575m, 3210s, 1618m, 1440m, 1313w, 1234w, 1112w, 969w, 824w, 755m, 655w.

[Zn(4-PyBim)$_2$(H$_2$O)$_2$(NO$_3$)$_2$] (9). The complex was prepared in the same way as was **7** except that the mixed MeCN−MeOH solution was used instead of CH_3COCH_3(5 mL) and $Zn(NO_3)_2\cdot 6H_2O$ (0.028 g, 0.1 mmol) was used instead of $Co(NO_3)_2\cdot 6H_2O$. Anal. calcd for $C_{24}H_{22}N_8O_8Zn$: C, 46.81; H, 3.60; N, 18.19. Found: C, 46.61; H, 3.63; N, 18.28%. IR (KBr, cm^{-1}): 3509m, 3219m, 1619m, 1381s, 1125w, 1022w, 829m, 755m.

[Cu$_2$(3-PyBim)$_2$(OAc)$_4$] (10). A solution of $Cu(OAc)_2\cdot H_2O$ (0.02 g, 0.1 mmol) in CH_3CN(2 mL) was layered onto a solution of 3-PyBim (0.02 g, 0.1 mmol) in mixed $CHCl_3-CH_3OH$ (5 mL, v/v = 1:1) in a test tube. The solution was left to stand for several weeks at room temperature, and green crystals were obtained. Anal. calcd for $C_{16}H_{15}CuN_3O_4$: C, 50.99; H, 4.01; N, 11.15. Found: C, 49.68; H, 4.05; N, 10.72%. IR (KBr, cm^{-1}): 3418m, 3179m, 1619s, 1429s, 1205w, 1130w, 1039m, 959w, 817w, 743m, 691m.

Table 2. Selected Bond Distances (Å) and Angles (deg) for Complexes 1–4

	1	2	3	4
Bond Distances				
Ag(1)−N(2)	2.1565(17)	2.162(3)	2.135(4)	2.174(3)
Ag(1)−N(1A)	2.1748(17)	2.195(3)	2.184(4)	2.197(3)
Bond Angles				
N(2)−Ag(1)−N(1A)	157.99(7)	154.12(11)	157.91(16)	154.07(13)
C(6)−N(2)−Ag(1)	129.92(14)	130.7(2)	128.1(3)	132.1(2)
C(12)−N(2)−Ag(1)	123.15(14)	123.6(2)	126.3(4)	121.1(2)
C(5)−N(1)−Ag(1A)	120.57(14)	119.1(2)	122.3(3)	117.4(3)
C(1)−N(1)−Ag(1A)	120.58(15)	123.0(2)	119.0(3)	126.8(3)

X-ray Crystallography. Experimental details of the X-ray structural analysis as well as the crystallographic data are provided in Table 1. Selected bond distances and angles are listed in Tables 2 and 3. The diffraction data were collected on a Siemens P4 four-cycle diffractometer for complexes **2**, **4**, **6**, and **8** or a Bruker Smart 1000 CCD diffractometer for complexes **1**, **3**, **5**, **7**, **9**, and **10** with

Table 3. Seclected Bond lengths (Å) and Angles (deg) for Complexes 5–10

5		
Ag(1)−N(1) 2.169(2)	Ag(1)−N(3) 2.219(2)	Ag(1)−O(1W) 2.595(3)
N(1)−Ag(1)−N(3) 151.21(9)	N(1)−Ag(1)−O(1W) 114.40(9)	N(3)−Ag(1)−O(1W) 89.39(10)
6		
Cu(1)−O(1) 1.948(2)	Cu(1)−N(1) 1.997(2)	
O(1)−Cu(1)−O(1) 180.00(18)	O(1)−Cu(1)−N(1) 91.37(10)	O(1)−Cu(1)−N(1) 88.63(10)
N(1)−Cu(1)−N(1) 180.00(19)		
7		
Co(1)−O(4) 2.068(2)	Co(1)−O(5) 2.073(2)	Co(1)−N(1) 2.172(2)
O(4)−Co(1)−O(5) 91.48(11)	O(4)−Co(1)−O(5) 88.52(11)	O(4)−Co(1)−N(1) 90.27(9)
O(4)−Co(1)−N(1) 89.73(9)	O(5)−Co(1)−N(1) 88.96(9)	O(5)−Co(1)−N(1) 91.04(9)
8		
Cu(1)−N(1) 2.0031(19)	Cu(1)−Cl(1) 2.3451(7)	
N(1)−Cu(1)−N(1) 180.00(11)	N(1)−Cu(1)−Cl(1) 89.91(6)	N(1)−Cu(1)−Cl(1) 90.09(6)
Cl(1)−Cu(1)−Cl(1) 180.00(4)		
9		
Zn(1)−N(1) 2.1046(13)	Zn(1)−O(4) 2.1254(12)	Zn(1)−O(3) 2.1904(12)
N(1)−Zn(1)−N(1) 180.0	N(1)−Zn(1)−O(4) 91.36(5)	N(1)−Zn(1)−O(4) 88.64(5)
O(4)−Zn(1)−O(4) 180.00(7)	N(1)−Zn(1)−O(3) 86.59(5)	N(1)−Zn(1)−O(3) 93.41(5)
O(4)−Zn(1)−O(3) 78.87(5)	O(4)−Zn(1)−O(3) 101.13(5)	O(3)−Zn(1)−O(3) 180.0
10		
Cu(1)−O(2) 1.9584(17)	Cu(1)−O(1) 1.9617(17)	Cu(1)−O(3) 1.9820(16)
Cu(1)−O(4) 1.9983(16)	Cu(1)−N(1) 2.1755(19)	
O(2)−Cu(1)−O(1) 167.83(7)	O(2)−Cu(1)−O(3) 90.15(8)	O(1)−Cu(1)−O(3) 89.38(8)
O(2)−Cu(1)−O(4) 88.46(8)	O(1)−Cu(1) O(4) 89.45(8)	O(3)−Cu(1)−O(4) 167.93(7)
O(2)−Cu(1)−N(1) 97.87(7)	O(1)−Cu(1)−N(1) 94.30(7)	O(3)−Cu(1)−N(1) 93.96(7)
O(4)−Cu(1)−N(1) 98.11(7)	O(2)−Cu(1)−Cu(1) 86.89(5)	

Scheme 1. Two Types of Coordination Modes for the PyBim Ligands

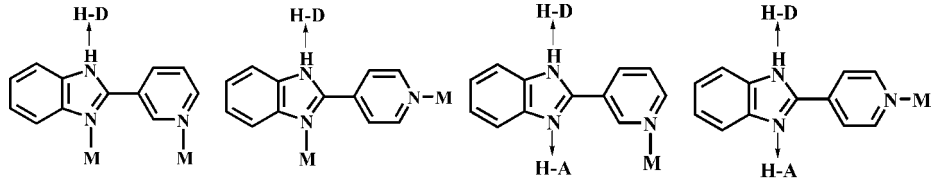

graphite-monochromated Mo Kα radiation ($\lambda = 0.71073$ Å) at room temperature. The Siemens P4 diffractometer was run using CAD4 Express Software,[12] and the data were processed by the program XCAD-4;[13] meanwhile, the Bruker Smart 1000 CCD diffractometer was run using the program SMART,[14] and the data were processed by SAINT+.[15] Absorption corrections were applied whenever it is necessary with psi-scan for four-cycle diffractometer and with the SADABS program[16] for the CCD diffractometer. The structures were solved by the direct methods (SHELXS) and refined by the full-matrix least-squares method against F_o^2 using the SHELXTL software.[17] The coordinates of the non-hydrogen atoms were refined anisotropically. All hydrogen atoms were introduced in calculated positions and refined with fixed geometry with respect to their carrier atoms.

Results and Discussion

Coordination Modes. The same feature of the ligands 3-PyBim and 4-PyBim is that they both have three types of nitrogen atoms: the imino nitrogen atom N_{Py} on the pyridyl ring, as well as the imino nitrogen atom N_{Bim} and the tertiary amino nitrogen atom HN_{Bim} on the benzimidazole ring. The imino N_{Py} and N_{Bim} atoms can directly coordinate with the metal ions while the HN_{Bim} group can behave as a hydrogen bonding donor. As shown in Scheme 1, there are two kinds of coordination modes depending on how many nitrogen atoms are involved in coordination. In the "end-to-end" fashion, the ligands act as bridges to join two metal ions, while in the "end-on" fashion the ligands are monodentate. As a consequence, the end-to-end mode leaves the HN_{Bim} group free to behave as a hydrogen-bond donor (H-D), while the end-on mode offers both a hydrogen-bond donor (N_{Bim}) and acceptor (H-A, N_{Bim}). Therefore, these two ligands provide versatile coordination and weak interaction sites for the construction of supramolecular assemblies. In addition, the ligands 3-PyBim and 4-PyBim are a pair of positional isomers which differ in position of N_{Py} atom with respect to N_{Bim} and HN_{Bim} atoms. This difference will cause different coordination directions when the ligands take the end-to-end coordination mode as shown in Scheme 1. Meanwhile, such a position difference will also result in different hydrogen-bond formation orientation in either end-to-end or end-on situations. For the present ten complexes, the ligands take the "end-to-end" mode in complexes **1**–**5**, while taking the "end-on" mode in complexes **6**–**10**.

Crystal Structure of the Basic Units. The molecular structures of complexes **1**–**4** are quite similar, consisting of a dinuclear M_2L_2 dication and weakly interacting anions. The cationic motif $[Ag_2(3\text{-PyBim})_2]^{2+}$ of complex **1** is depicted

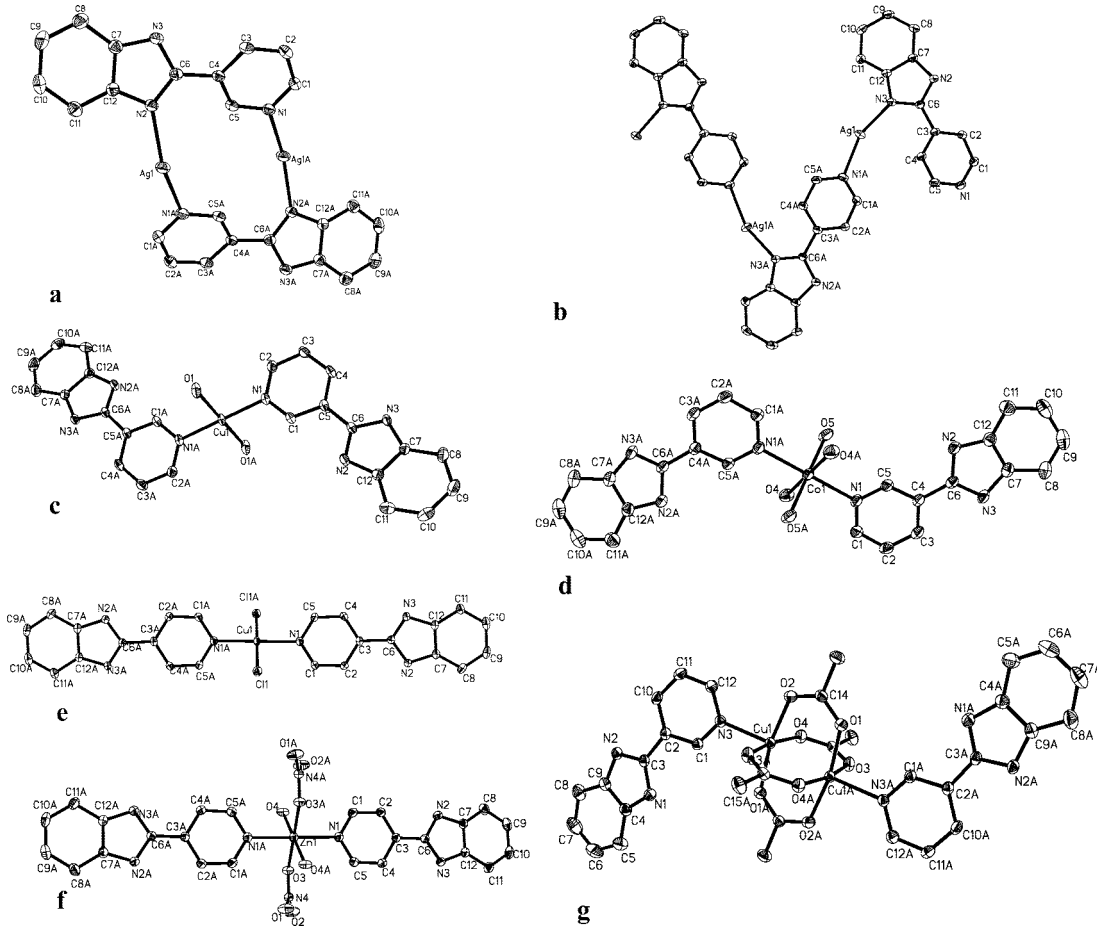

Figure 1. Molecular structures of complexes with atomic labeling scheme at the 30% probability level: (a) **1**–**4**, (b) **5**, (c) **6**, (d) **7**, (e) **8**, (f) **9**, and (g) **10**.

in Figure 1a as a representative example, and the seclected bond lengths and angles for complexes **1**−**4** are shown in Table 2.

The common structural character of the cationic motifs in complexes **1**–**4** is that two Ag (I) atoms are bridged by two 3-PyBim ligands to form an $[Ag_2(PyBim)_2]^{2+}$ metallacycle, in which every Ag atom is almost linearly coordinated by the N_{py} atom from the pyridyl of one ligand and the N_{Bim} atom from the benzimidazolyl of the other. The 3-PyBim ligands take the end-to-end mode and leave the NH group on benzimidazolyl open as an effective hydrogen-bond donating position. Therefore, abundant hydrogen bonds can be formed between the NH groups and the counteranions, such as BF_4^-, NO_3^-, ClO_4^-, and $CF_3SO_3^-$ in complexes **1**–**4**, respectively. By contrast, when silver nitrate reacts with the isomeric ligand 4-PyBim, although the Ag(I) atoms are still two coordinated and the ligand 4-PyBIm takes the same end-to-end coordination mode, a one-dimensional zigzag chain instead of the cyclic units is formed in complex **5** as shown in Figure 1b. This is obviously due to a larger coordinating angle between N_{Py} and N_{Bim} atoms compared to those of the ligand 3-PyBim. The Ag-N_{Bim} (2.169(2) Å) distance is slightly shorter than that of Ag-N_{Py} (2.219(2) Å) as listed in Table 3, similar to those observed in complexes **1**–**4** and other related structures.[9a] On the other hand, the X-ray structural analysis also reveals a water molecule attached to an Ag(I) atom, and the distance (Ag(1)−O(1W) = 2.595(3) Å) falls into the range of weak coordination interactions. Therefore, such a 1D chain structure can provide both NH and OH groups for the formation of hydrogen bonds.

In contrast to the Ag(I) complexes **1**–**5**, all other metal ions, including Cu(II), Co(II), and Zn(II) in complexes **6**–**10**, are only coordinated by N_{Py} atoms with either the 3-PyBim or 4-PyBim ligand taking the end-on coordination mode as seen in Figure 1c−g. Therefore, both the N_{Bim} and HN_{Bim} groups on a benzimidazolyl ring are uncoordinated and can act as potential hydrogen-bond donors and acceptors, respectively.

The asymmetric unit of complex **6,** $[Cu(3\text{-}PyBim)_2(H_2O)_2](ClO_4)_2$, contains one Cu(II) ion, one 3-PyBim ligand, one coordinated water molecule, and one uncoordinated ClO_4^- group. The local coordination geometry around the Cu(II) center can be described as a square as shown in Figure 1c. The Cu−O and Cu−N bond distances are normal and the bond angles around the Cu(II) center are close to the orthogonal requirement as listed in Table 3. The Cu(II) ion is coordinated by the pyridyl nitrogen atom N_{Py} rather than the benzimidazolyl nitrogen atom N_{Bim}, probably due to the steric congestion around the N_{Bim} atom. Complex **7**, $[Co(3\text{-}PyBim)_2(H_2O)_4](NO_3)_2\cdot(H_2O)_4$, also shows a mononuclear basic unit (Figure 1d) but contains four coordinated water molecules, four solvated water molecules, and two uncoordinated NO_3^- groups. Thus, the octahedron coordination geometry CoN_2O_4 is formed by four aqua oxygen atoms and two N_{Py} nitrogen atoms from two independent 3-PyBim ligands. In complex **8**, there is one crystallographically unique Cu(II) ion, one 4-PyBim ligand, one water molecule, and one chlorine atom. As shown in Figure 1e, the Cu(II) ion exhibits a square coordination environment comprising two N_{Py} nitrogen atoms and two chlorine atoms. The coordination environment of the central metal ion of complex **9** is similar to that reported by

Table 4. Selected Details of the Hydrogen Bonds in Complexes 1–10

	symmetry code	d(D−H), Å	d(H···A), Å	d(D···A), Å	∠D−H···A, deg
		1			
N3−H3B···F3	$1 + x$, $^1/_2 - y$, $^1/_2 + z$	0.86	2.07	2.847(2)	150.7
		2			
N3−H3A···O3	x, $1 + y$, z	0.86	2.00	2.852(4)	171.4
N3−H3A···O2	x, $1 + y$, z	0.86	2.58	3.145(4)	124.0
		3			
N3−H3A···O3	$-x - 1$, $-y - 1$, $1 - z$	0.86	2.17	3.015(6)	169.4
		4			
N3−H3A···O1	x, $-y - ^1/_2$, $z - ^1/_2$	0.86	1.99	2.832(4)	166.3
		5			
N2−H2A···O1	x, y, z	0.86	2.04	2.894(3)	170.2
N2−H2A···O3	x, y, z	0.86	2.56	3.210(3)	133.0
O1W−H2···O1	x, y, $z - 1$	0.77(5)	2.23(5)	2.970(4)	164(5)
O1W−H1···O2	$-x$, $1 - y$, $z - 1$	0.85(5)	2.02(5)	2.855(5)	165(4)
		6			
N2−H2N···O12	$1 - x$, $-y$, $-z$	0.85(3)	2.09(3)	2.926(4)	168(3)
O1−H2O···O13	x, y, $z + 1$	0.78(4)	2.07(4)	2.841(5)	171(4)
O1−H1O···N3	$1 - x$, $y - ^1/_2$, $-z + ^1/_2$	0.84(5)	1.83(5)	2.653(3)	164(5)
		7			
O4−H4C···O6	x, y, z	0.82	1.86	2.668(4)	168.5
O5−H5C···O7	$1 - x$, $-y$, $-z$	0.82	1.96	2.722(3)	153.2
N2−H2B···O2	$1 - x$, $-y$, $-z$	0.86	2.02	2.859(4)	165.3
O4−H4B···O3	x, y, z	0.76(4)	2.03(4)	2.777(4)	171(4)
O5−H5B···O7	x, y, z	0.73(4)	2.04(4)	2.753(4)	168(4)
O6−H62···O3	$-x$, $1 - y$, $-z$	0.74(5)	2.20(5)	2.919(5)	165(5)
O6−H61···O2	$x - 1$, y, z	0.83(5)	2.05(5)	2.868(5)	168(5)
O7−H71···N3	x, y, $z + 1$	0.851(19)	1.93(2)	2.771(3)	169(4)
		8			
N2−H21···Cl1	x, $-y + ^1/_2$, $z + ^1/_2$	0.79(3)	2.46(3)	3.197(2)	156(3)
O1−H02···N3	$-x$, $y + ^1/_2$, $-z + ^1/_2$	0.90(5)	1.96(5)	2.848(3)	169(4)
		9			
O4−H4A···O1	$1 - x$, $2 - y$, $-z - 1$	0.82	2.07	2.8159(19)	150.5
N2−H2A···O2	x, y, $z + 1$	0.86	2.09	2.9233(19)	162.0
O4−H4C···N3	x, $y + 1$, z	0.76(2)	2.09(2)	2.8380(18)	170(2)
		10			
N3−H3A···O4	$-x$, $3 - y$, $-z$	0.86	2.03	2.825(3)	153.3

Lin,[9c] in which a distorted octahedral geometry is formed around Zn(II) comprised of two N_{Py} atoms from two 4-PyBim ligands, two O atoms from two nitrate groups, and another two O atoms from two water molecules. A dinuclear structural unit is formed in complex **10** by using $Cu(CH_3CO_2)_2$ as the metal source. As shown in Figure 1g, the Cu(II) center is defined by four oxygen atoms of four different carboxylate groups and one N_{Py} atom of the 3-PyBim ligand. Two Cu(II) centers are bridged by four μ-AcO^- groups over a metal−metal separation of 2.6435(5) Å, offering the well-known paddle-wheel dimetal subunit.

In general, the basic structural units formed in complexes **6–10** exhibit a linear arrangement of two 4-PyBim ligands while "Z" type arrangement of two 3-PyBim ligands due to positional isomerization. All of them provide multiple hydrogen bonding sites and weak M−O interaction sites ready for assembly into higher dimensions via these intermolecular interactions. Therefore, these structural units give rise to versatile supramolecular synthons for formation of extended structures.[18]

Crystal Packing and Dimension Increase. As described above, all the structural units are zero-dimensional, except that complex **10** shows 1D structure. During crystallization, a balance between the adaptability of these structural units and the synergistic effects of various weak interactions has to be achieved. In other words, it is important to understand how these basic units are interacting to pack in the crystal. Since each crystal is believed to be an excellent supermolecule,[19] the crystal-packing mode can be easily analyzed by means of decoding the solid network, whose construction strongly depends on influencing factors such as the numbers and orientations of interaction sites, as well as influences from counteranions and solvents. Among these factors, the hydrogen bonds are the main forces to hold the subunits together and sustain the crystal framework, while the $\pi-\pi$ interactions normally play important roles to direct the stacking fashion. To conveniently clarify the overal crystal structures in a dimension increasing way by considering the propagation of the basic structural units via intermolecular interactions, we will regard the hydrogen bonding and weak coordination interaction as intermolecular connections but consider $\pi-\pi$ interaction as a crystal packing contribution. The main hydrogen bonds parameters for complexes **1–10** are listed in Table 4.

In complex **1**, every two adjacent $[Ag_2(PyBim)_2]^{2+}$ units are connected by a couple of complementary N−H···F hydrogen bonds formed between the HN_{Bim} group and BF_4^- and Ag···F interactions (2.780(2) Å) as shown in Figure 2, thus resulting in a 1D chain structure extending along the a axis. Similarly, in complex **2**, the N−H···O hydrogen bonds between HN_{Bim} group and NO_3^- and the Ag···O interactions (2.682(4) Å) join $[Ag_2(PyBim)_2]^{2+}$ units to give a 1D chain. But, these 1D chains are further connected by the second type

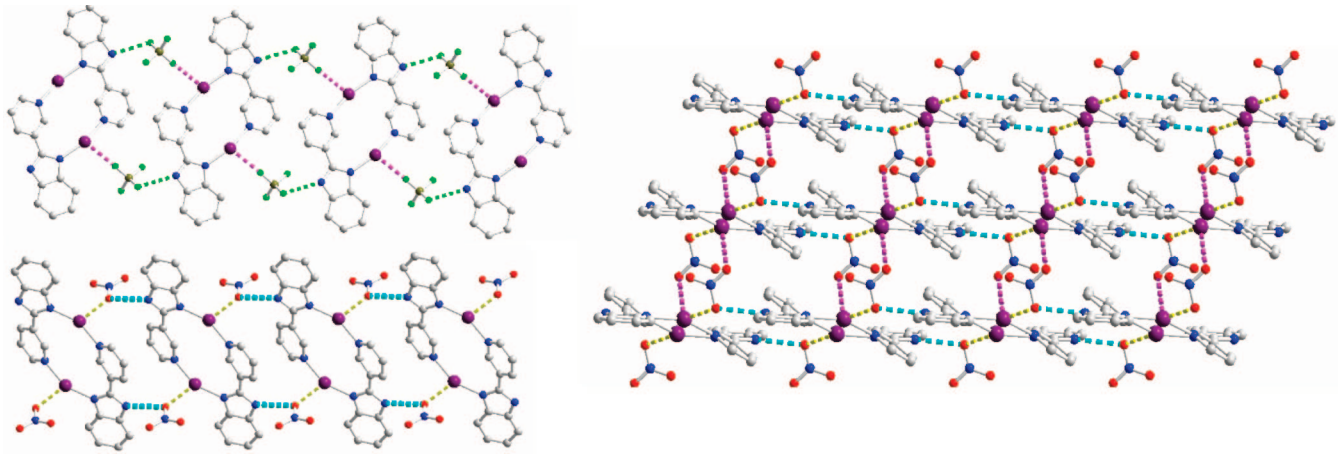

Figure 2. One-dimensional chain structures in **1** formed via N−H···F hydrogen bonds and weak Ag···F interactions (left upper) and those in **2** formed via N−H···O hydrogen bonds and weak Ag···O interactions (left lower) and 2D sheet in **2** formed via the second type of Ag···O interactions between adjacent 1D chains (right; different interactions are distinguished by different colors).

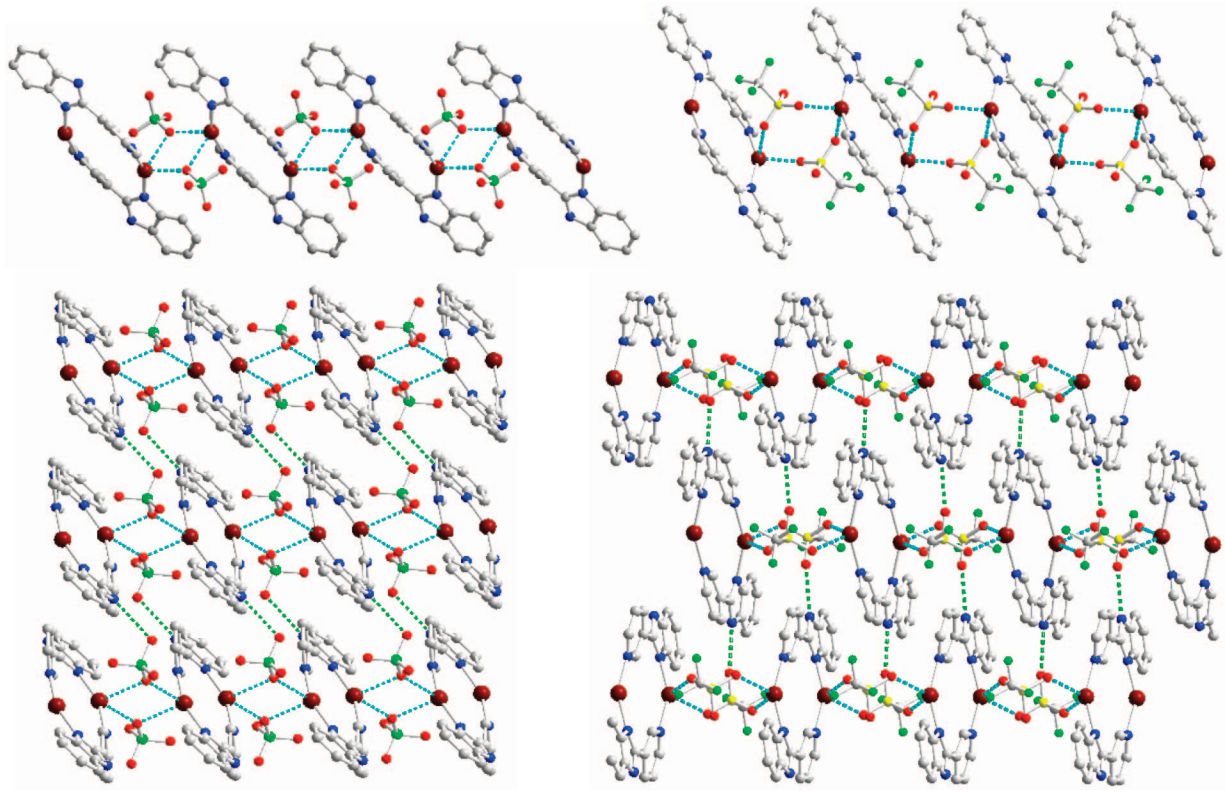

Figure 3. One-dimensional chain structures in **3** (left) and **4** (right) formed via weak Ag···O interactions (upper) and 2D sheet formed via N−H···O hydrogen bonds between adjacent 1D chains (lower).

of intermolecular Ag···O interactions (2.783(3) Å) to give rise to a 2D sheet as shown in Figure 2. Therefore, the 1D chains in complex **2** are stacked in parallel via offset $\pi-\pi$ interactions, while those in complex **1** show herringbone packing fashion sustained by C−H···π interactions.

The crystal structures of complexes **3** and **4** have been previously discussed in a communication.[9b] The 1D chain structures are formed via weak Ag···O interactions (2.760(3), **3**, and 2.570(3) Å, **4**) as shown in Figure 3. Such 1D chains are further connected by N−H···O hydrogen bonds between HN_{Bim} groups and ClO_4^- or $CF_3SO_3^-$ anions to lead to 2D sheets. However, the aromatic stacking modes in complexes **3** and **4** are different. In **3**, the Bim rings display a head-to-tail packing fashion, while in **4** the ligands exhibit a face-to-face packing fashion.

It is clear that, since essentially the same $[Ag_2(PyBim)_2]^{2+}$ units are formed in complexes **1**–**4**, the intermolecular connecting fashions in these complexes are comparable. However, the crystal packing fashions are distinguished by the counteranions. Although the structural units show similar chainlike connectivity, the aromatic rings are stacked in varied ways in dependence on the anions.

In complex **5**, the use of the 4-PyBim isomer affords a chain structure in contrast to the cyclic motifs in complexes **1**–**4**.

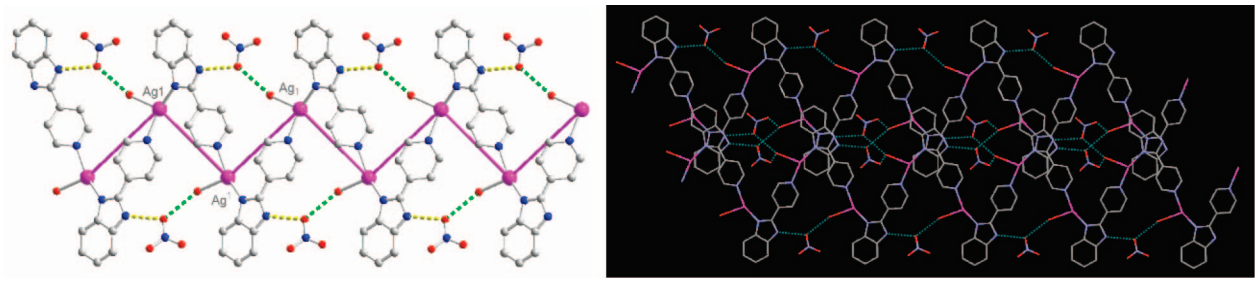

Figure 4. One-dimensional zig-zag chain (denoted by the bold pink line) directed by intramolecular hydrogen bonds (left) and a 2D sheet formed via intermolecular hydrogen bonds in complex **5** (right).

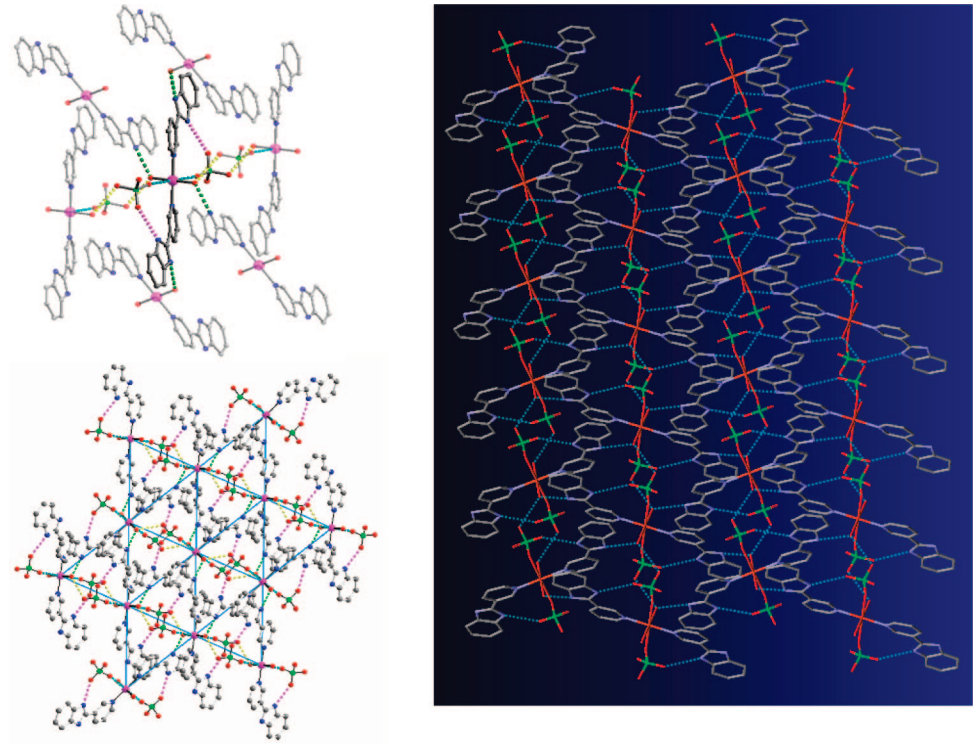

Figure 5. Four types of interactions (shown in different colors) formed in complex **6** (upper left) with each unit connecting six neighbors to give a (3,6) topology (upper right, shown in blue solid line), thus forming a 2D layer (lower) in the *bc* plane.

Crystal analysis reveals that such a zigzag chain arrangement is sustained further by two types of intramolecular hydrogen bonds (Figure 4): the N−H···O hydrogen bonds between HN_{Bim} group and one O atom of NO_3^- and the O−H···O hydrogen bonds between the H_2O molecule and the same O atom of NO_3^-. The water molecule itself weakly interacts with the Ag(I) ion. Therefore, there are three kinds of intrachain interactions: N−H···O, O−H···O, and Ag···O. In addition, The second type of O−H···O hydrogen bonds are formed between the water molecule and the NO_3^- group belonging to the adjacent chains, which link the 1D chains into a 2D sheet as seen in Figure 4. The $\pi-\pi$ interactions are formed between the 1D chains stacked in a parallel fashion.

The completely different structural units formed in complexes **6**–**9** cause fairly different dimension-increase methods compared with those in **1**–**5**. The formation of monomeric building units leaves N_{Bim} free to act as hydrogen bonding acceptor. In the meantime, the remaining coordination sites of metal ions are occupied by water molecules which offer more potential hydrogen-bond donors and acceptors. In complex **6**, all the 3-PyBim ligands, coordinating water molecules, and ClO_4^- anions are involved in supramolecular interactions which can be classified into four types, as shown in Figure 5: the Cu···O weak interaction (2.518(3) Å) between the $[Cu(3\text{-}PyBim)_2(H_2O)_2]^{2+}$ cation and two ClO_4^- anions, the O−H···O and O−H···N hydrogen bonds formed between the coordinated water molecule and one O atom of ClO_4^- and the N_{Bim} atom of the ligand, and the N−H···O hydrogen bonds between the HN_{Bim} group and another O atom of ClO_4^- anion. Each $[Cu(3\text{-}PyBim)_2(H_2O)_2]^{2+}$ cationic unit is linked to six adjacent structural units via these four types of interactions, thus forming a (3,6) topologic connectivity and leading to 2D layer packing in the *bc* plane as depicted in Figure 5. The $\pi-\pi$ interactions are observed in between the aromatic rings inside the 2D layer, but no obvious aromatic stacking is formed between the 2D layers.

An even more complicated supramolecular interaction system is found in complex **7**, $[Co(3\text{-}PyBim)_2(H_2O)_4](NO_3)_2\cdot(H_2O)_4$, which comprises four coordinated and four solvated water molecules and two uncoordinated NO_3^- groups. Detailed crystal network decoding analysis revealed a 1D chain structure involving all the coordinated and noncoordinated molecules as shown in Figure 6. This 1D chain is assembled by solvated water molecules and NO_3^- groups via formation of multiple N−H···O

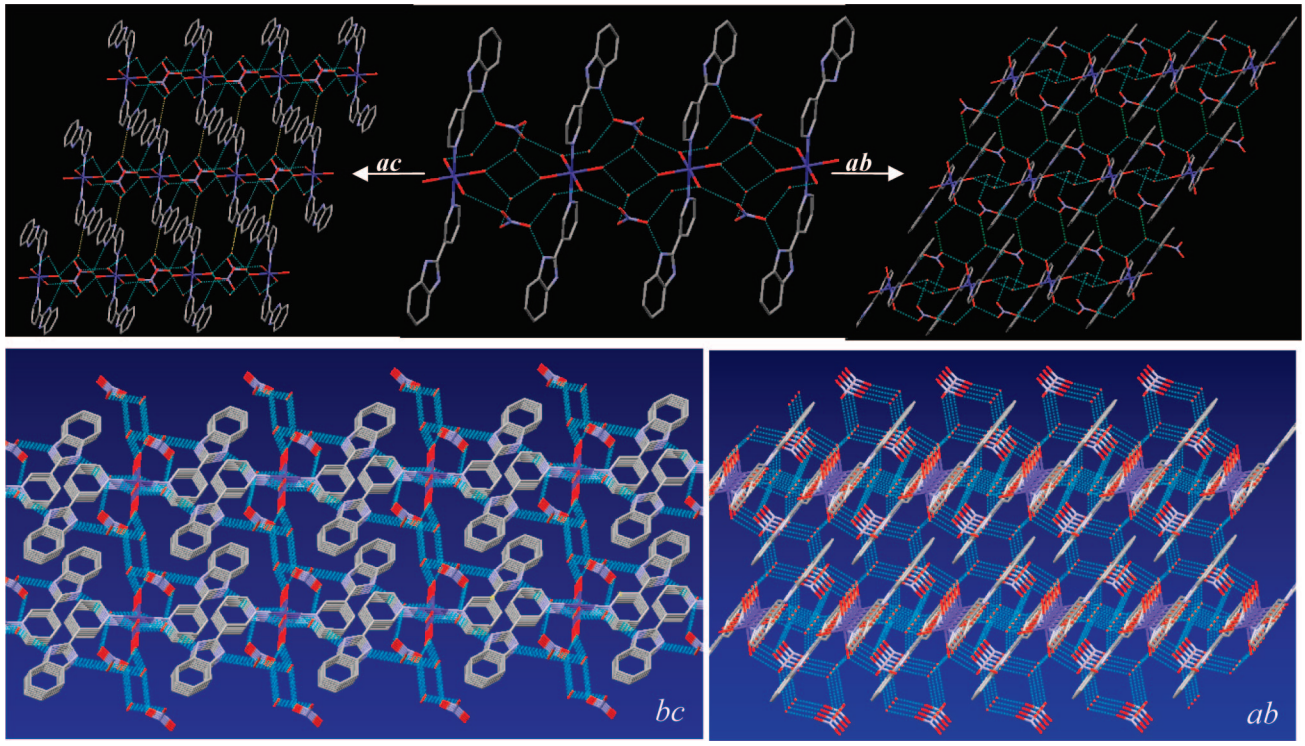

Figure 6. Hydrogen-bonded framework in complex **7**: 1D chain structure formed via multiple hydrogen bonds and propagation via N−H···O hydrogen bonds (yellow) in the *ac* plane and O−H···O hydrogen bonds (green) in the *ab* plane (upper), resulting in 3D frameworks viewed in the *a* and *c* directions (lower).

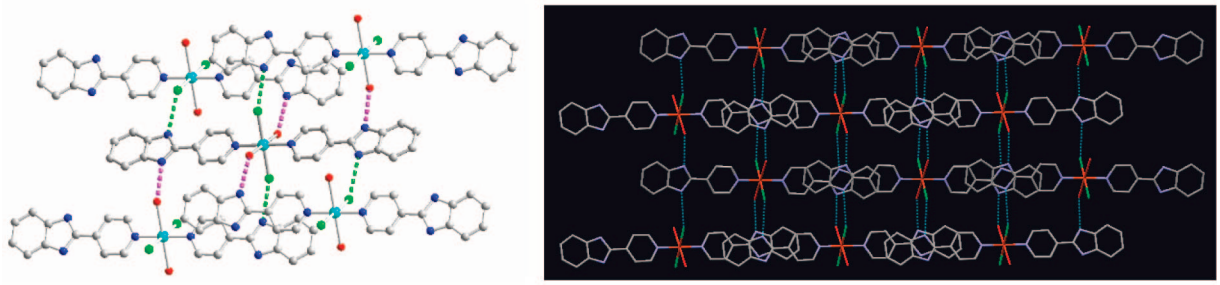

Figure 7. N−H···Cl and O−H···N hydrogen bonds (highlighted in different colors) formed between structural units in complex **8** (left) and a 2D sheet formed with these hydrogen bonds (right).

and O−H···O hydrogen bonds with the $[Co(3\text{-}PyBim)_2(H_2O)_4]^{2+}$ cationic units. In total, 14 hydrogen bonds are formed between every two cationic units, resulting in one four-membered O4, two seven-membered CoNO5, and two eight-membered CoNO6 hydrogen-bonded rings. On the basis of this 1D chain, the dimension increase of the solid network can be described as follows: (1) in the *ac* plane, the N−H···O hydrogen bonds between the HN_{Bim} group and one water molecule extend the chain structure into a 2D sheet; (2) in the *ab* plane, the O−H···O hydrogen bonds formed between water molecules and NO_3^- anions make up a ribbon to join the chains into a 2D sheet, too. Therefore, the overall crystal packing is consolidated by multiple hydrogen bonds, leading to a 3D network as shown in Figure 6 in different directions. The offset $\pi-\pi$ interactions are formed between the aromatic rings.

By changing the ligand from 3-PyBim to 4-PyBim, the monomeric structural units give a more regular linear arrangement of the ligands and, therefore, a much simplified intermolecular connectivity. As shown in Figure 7, complex $[Cu(4\text{-}PyBim)_2(Cl)_2](H_2O)_2$ (**8**) displays only two types of hydrogen bonds: the N−H···Cl between HN_{Bim} and the Cl^- anion and the O−H···N between N_{Bim} and the H_2O molecule. These two types of hydrogen bonds connect the neutral $[Cu(4\text{-}PyBim)_2(Cl)_2]$ structural units together with the Cu···O weak interactions between the Cu(II) ion and water molecule to give rise to a 2D layer extending in the *bc* plane. The head-to-tail $\pi-\pi$ interactions are formed between the adjacent monomeric units, thus sustaining a parallel packing of the 2D layres.

In complex $[Zn(4\text{-}PyBim)_2(H_2O)_2(NO_3)_2]$ (**9**), similar linear building units are formed but the NO_3^- anion offers more oxygen atoms involved in hydrogen bonding compared with the sole Cl^- anion in complex **8**. Nevertheless, the intermolecular connectivity is still much simpler in comparison with that in complexes **6** and **7** exhibiting *Z* type conformation of the structural units. As shown in Figure 8, a 2D sheet in the *bc* plane is formed via the N−H···O hydrogen bonds between the HN_{Bim} group and one O atom of the NO_3^- anion and the O−H···N hydrogen bonds between the water molecule and N_{Bim} atom. While in the *ac* plane, the above N−H···O hydrogen bonds together with the O−H···O hydrogen bonds between

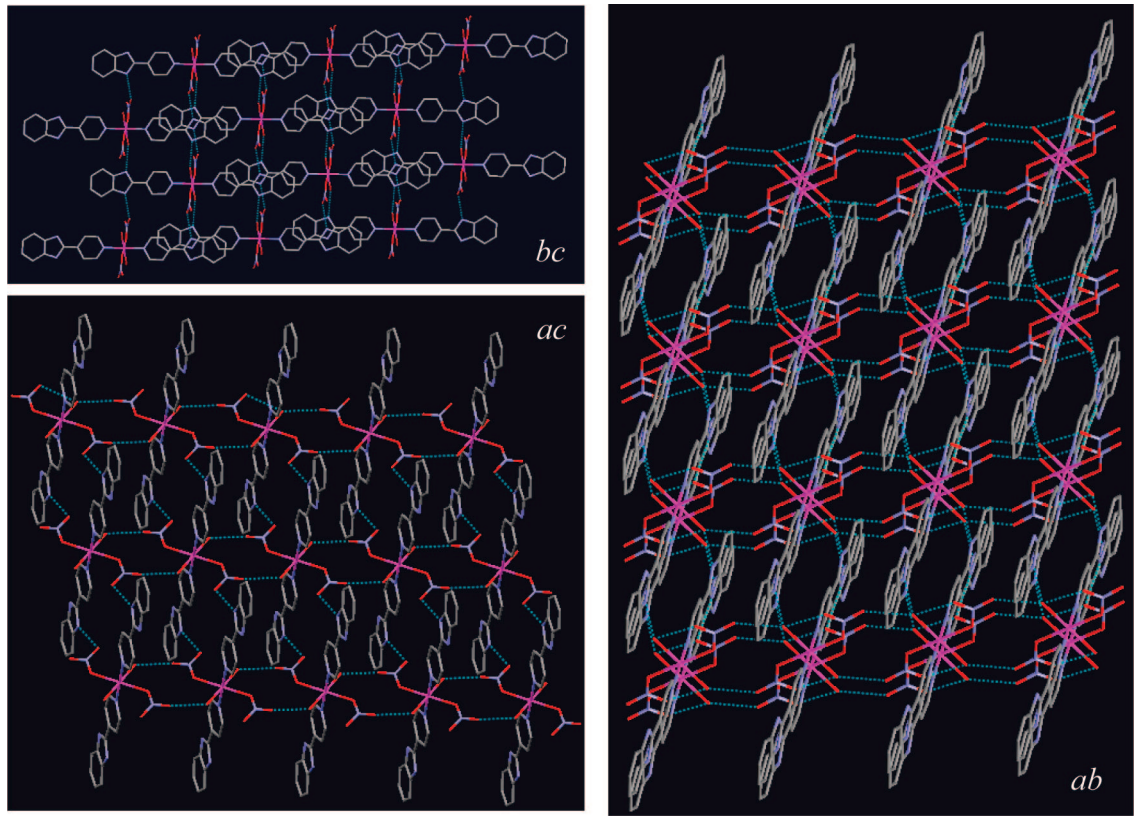

Figure 8. O−H···N, O−H···O, and N−H−O hydrogen-bonded 2D sheets in the *bc* and *ac* planes (left) and a 3D framework viewed in the *c* direction (right) in complex **9**.

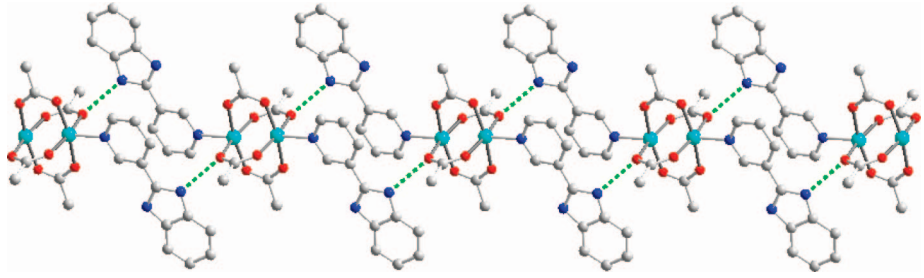

Figure 9. 1D chain structure in complex **10** formed via N−H···O hydrogen bonds.

the water molecule and the NO_3^- anion sustain a 2D sheet too. Therefore, a 3D network structure is assembled from these three types of hydrogen bonds which determine the crystal packing as shown in Figure 8. Similarly in complex **8**, the head-to-tail $\pi-\pi$ interactions are formed between the adjacent monomeric units.

In comparison to complexes **1**–**9**, the structural unit of complex **10** is a dinuclear motif with all coordination sites occupied by four carboxylate groups. There is not any water molecule in the crystal; therefore, only one type of hydrogen bond is present: the N−H···O hydrogen bonds formed between the HN_{Bim} group and one O atom of a CH_3COO^- anion, resulting in a 1D chain as shown in Figure 9. The face-to-face $\pi-\pi$ interactions are formed between these 1D chains, which stabilize the overal crystal packing.

Thermogravimetric Analysis. Thermogravimetric (TG) analysis in air under 1 atm of pressure at a heating rate of 10 °C min^{-1} was performed on polycrystalline samples for complexes **8** and **10**. For complex **8**, the weight loss of 6.5% before 245 °C is equivalent to the loss of the two water molecules per formula unit (calcd = 6.42%). Two major weight losses occur after 300 °C (see Figure S1 in the Supporting Information). The thermal gravimetric analysis (TGA) diagram of complex **10** reveals two distinct weight loss regions centered around 215 and 350 °C. The structure shows relatively lower thermal stability compared to that of complex **8**.

Conclusions

In summary, two isomeric ligands, 3-PyBim and 4-PyBim, were found to coordinate with the Ag(I) ion in an end-to-end coordination mode and in an end-on one with other metal ions, leading to diversified basic structural units including monomeric, dinuclear, dimetal cyclic and chain motifs. Different coordination modes of the ligands and environments around the metal ions offer distinctive supramolecular interaction sites and fashions for each kind of structural unit. Therefore, each complex has its specific unit-connectivity and crystal-packing mode. The 1D (**1**, **10**), 2D (**2**–**6**, **8**) or 3D (**7**, **9**) frameworks were classified in their method of dimension-increase to aid hydrogen bonding and M−O weak interactions. The $\pi-\pi$ interactions also play an important role in stablizing the resulting crystal packing. This suggests that the rational analysis of crystal packing and supramolecular interactions in a series of structur-

ally related complexes could be helpful in understanding the subtle roles played by various dative and nondative bonds and, finally, in approaching the ambitious goal to engineer crystal.

Acknowledgment. This work was supported by the National Science Funds for Distinguished Young Scholars of China (Grant 20525310), the 973 Program of China (Grant 2007CB815302), the NSF of China (Grants 20673147, 20773167, 20731005), and the RFDP of Higher Education.

Supporting Information Available: X-ray crystallographic data in CIF format, TGA curves of **8** and **10**, and XRD patterns for **2**, **8**, and **10**. This material is available free of charge via the Internet at http://pubs.acs.org.

References

(1) (a) Desiraju, G. R. *Angew. Chem., Int. Ed. Engl.* **1995**, *34*, 2311. (b) Braga, D.; Brammer, L.; Champness, N. R. *Cryst. Eng. Commun.* **2005**, *7*, 1. (c) Brammer, L. *Chem. Soc. Rev.* **2004**, *33*, 476. (d) Braga, D. *Chem. Commun.* **2003**, 2751. (e) Hosseini, M. W. *Cryst. Eng. Commun.* **2004**, *6*, 318. (f) Holman, K. T.; Pivovar, A. M.; Swift, J. A.; Ward, M. D. *Acc. Chem. Res.* **2001**, *34*, 107. (g) Beatty, A. M. *Cryst. Eng. Commun.* **2001**, *3*, 243. (h) Kitagawa, S.; Kitauro, R.; Noro, S. *Angew. Chem., Int. Ed.* **2004**, *43*, 2334. (i) Janiak, C. *J. Chem. Soc., Dalton Trans.* **2000**, 3885. (j) James, S. L. *Chem. Soc. Rev.* **2003**, *32*, 276. (k) Eddaoudi, M.; Moler, D. B.; Li, H.; Chen, B.; Reineke, T. M.; O'Keeffe, M.; Yaghi, O. M. *Acc. Chem. Res.* **2001**, *34*, 319. (l) Evans, O. R.; Lin, W. *Acc. Chem. Res.* **2002**, *35*, 511.

(2) (a) Yang, W. B.; Lu, C. Z.; Lin, X.; Wu, C. D.; Wu, D. M.; Zhuang, H. H. *Inorg. Chem. Commun.* **2001**, *4*, 285. (b) Burchell, T. J.; Eisler, D. J.; Puddephatt, R. J. *Chem. Commun.* **2004**, 944. (c) Yue, W. M.; Bishop, R.; Craig, D. C.; Scudder, M. L. *Cryst. Eng. Commun.* **2002**, *4*, 591.

(3) (a) Su, C.-Y.; Yang, X.-P.; Kang, B.-S.; Mak, T. C. W. *Angew. Chem., Int. Ed.* **2001**, *40*, 1725. (b) Su, C.-Y.; Kang, B.-S.; Liu, H.-Q.; Wang, Q.-G.; Mak, T. C. W. *Chem. Commun.* **1998**, 1551. (c) Janiak, C. *J. Chem. Soc., Dalton Trans.* **2000**, 3885. (d) Liu, G.-F.; Ye, B.-H.; Ling, Y.-H.; Chen, X.-M. *Chem. Commun.* **2002**, 1442. (e) Bu, X.-H.; Chen, W.; Lu, S.-L.; Zhang, R.-H.; Liao, D.-Z.; Bu, W.-M.; Shionoya, M.; Brisse, F.; Ribas, J. *Angew. Chem., Int. Ed.* **2001**, *40*, 3301. (f) Dong, Y.-B.; Zhao, X.; Tang, B.; Wang, H.-Y.; Huang, R.-Q.; Smith, M. D.; zur Loye, H.-C. *Chem. Commun.* **2004**, 220.

(4) (a) Tynan, E.; Jensen, P.; Kruger, P. E.; Lees, A. C. *Chem. Commun.* **2004**, 776. (b) Uemura, K.; Kitagawa, S.; Fukui, K.; Saito, K. *J. Am. Chem. Soc.* **2004**, *126*, 3817. (c) Wang, R. H.; Zhou, Y. F.; Sun, Y. Q.; Yuan, Q. D.; Han, L.; Lou, B. Y.; Wu, B. L.; Hong, M. C. *Cryst. Growth Des.* 20055, 251.

(5) Tidwell, R. R.; Jones, S. K.; Naiman, N. A.; Berger, L. C.; Brake, W. B.; Dykstra, C. C.; Hall, J. E. *Antimicrob. Agents Chemother.* **1993**, *37*, 1713.

(6) Santra, S.; Dogra, S. K. *J. Mol. Struct.* **1999**, *476*, 223.

(7) (a) Su, C.-Y.; Kang, B.-S.; Yang, Q.-C.; Mak, T. C. W. *J. Chem. Soc., Dalton Trans.* **2000**, 1857. (b) Matthews, C. J.; Broughton, V.; Bernardinelli, G.; Melich, X.; Brand, G.; Willis, A. C.; Williams, A. F. *New J. Chem.* **2003**, *27*, 354. (c) Moon, D.; Lah, M. S.; Sesto, R. E. D.; Miller, J. S. *Inorg. Chem.* **2002**, *41*, 4708. (d) Hammes, B. S.; Kieber-Emmons, M. T.; Sommer, R.; Rheingold, A. L. *Inorg. Chem.* **2002**, *41*, 1351.

(8) (a) Su, C.-Y.; Kang, B.-S.; Wang, Q.-G.; Mak, T. C. W. *J. Chem. Soc., Dalton Trans.* **2000**, 1831. (b) Su, C.-Y.; Kang, B.-S.; Du, C.-X.; Yang, Q.-C.; Mak, T. C. W. *Inorg. Chem.* **2000**, *39*, 4843. (c) Yang, X.-P.; Su, C.-Y.; Kang, B.-S.; Feng, X.-L.; Xiao, W.-L.; Liu, H.-Q. *J. Chem. Soc., Dalton Trans.* **2000**, 3253. (d) Yang, X.-P.; Kang, B.-S.; Wong, W.-K.; Su, C.-Y.; Liu, H.-Q. *Inorg. Chem.* **2003**, *42*, 169. (e) Chen, C.-L.; Su, C.-Y.; Xu, A.-W.; Zhang, H.-X.; Feng, X.-L.; Kang, B.-S. *Acta Crystallogr., Sect. E* **2002**, *58*, o916. (f) van Albada, G. A.; Veldman, N.; Spek, A. L.; Reedijk, J. *J. Chem. Cryst.* **2000**, *30*, 69. (g) Lü, X.-Q.; Pan, M.; He, J.-R.; Cai, Y.-P.; Kang, B.-S.; Su, C.-Y. *Cryst. Eng. Commun.* **2006**, *8*, 827. (h) Lü, X.-Q.; Qiao, Y.-Q.; He, J.-R.; Pan, M.; Kang, B.-S.; Su, C.-Y. *Cryst. Growth Des.* **2006**, *6*, 1910.

(9) (a) Xia, C. K.; Lu, C. Z.; Zhang, Q. Z.; He, X.; Zhang, J. J.; Wu, D. M. *Cryst. Growth Des.* **2005**, *5*, 1569. (b) Su, C.-Y.; Yang, X.-P.; Liao, S.; Mak, T. C. W.; Kang, B.-S. *Inorg. Chem. Commun.* **1999**, *2*, 383. (c) Wang, Z.-Y.; Wilson, S. R.; Foxman, B. M.; Lin, W.-B. *Cryst. Eng.* **1999**, *2*, 91.

(10) Carina, R. F.; Williams, A. F.; Bernardinelli, G. *Inorg. Chem.* **2001**, *40*, 1826.

(11) Huang, X. C.; Zhen, M. H.; Ng, S. W. *Acta Crystallogr., Sect. E* **2004**, *60*, o939.

(12) *CAD4 Express Software*; Enraf-Nonius: Delft, The Netherlands, 1994.

(13) Harms, K.; Wocadlo, S. *XCAD-4. Program for Processing CAD-4 Diffractometer Data*. University of Marburg: Germany, 1995.

(14) *SMART*, version 5.0; Bruker AXS: Madison, WI, 1998.

(15) *SAINT+*, version 6.0; Bruker AXS: Madison, WI, 1999.

(16) *SADABS, Bruker Nonius area detector scaling and absorption correction*, V2.05; Bruker AXS: Madison, WI, 1998.

(17) Sheldrick, G. M. *SHELX 97, Program for Crystal Structure Solution and Refinement*; Göttingen Unviersity: Germany, 1997.

(18) (a) Desiraju, G. R. *Chem. Commun.* **1997**, 1475. (b) Reddy, D. S.; Craig, D. C.; Desiraju, G. R. *J. Am. Chem. Soc.* **1996**, *118*, 4090. (c) Suksangpanya, U.; Blake, A. J.; Hubberstey, P.; Wilson, C. *Cryst. Eng. Commun.* **2002**, *4*, 552.

(19) (a) *Perspectives in Supramolecular Chemistry: The Crystal as a Supramolecular Entity*; Desiraju, G. R., Ed.; Wiley: Chichester, 1996; Vol. 2. (b) Braga, D. *J. Chem. Soc., Dalton Trans.* **2000**, 3705. (c) Moulton, B.; Zaworotko, M. J. *Chem. Rev.* **2001**, *101*, 1629. (d) Beatty, A. M. *Cryst. Eng. Commun.* **2001**, *51*, 1. (e) Blake, A. J.; Champness, N. R.; Hubberstey, P.; Li, W.-S.; Withersby, M. A.; Schröder, M. *Coord. Chem. Rev.* **1993**, *183*, 117.

CG070080J